

EMULSIFIED CHITOSAN-PLGA SCAFFOLDS FOR  
TISSUE ENGINEERING

By

ALIAKBAR MOSHFEGHIAN

Bachelor of Science in Chemical Engineering

Oklahoma State University

Stillwater, OK

2003

Submitted to the Faculty of the  
Graduate College of the  
Oklahoma State University  
in partial fulfillment of  
the requirements for  
the Degree of  
MASTER OF SCIENCE  
December, 2005

EMULSIFIED CHITOSAN-PLGA SCAFFOLDS FOR  
TISSUE ENGINEERING

Thesis Approved:

Dr. Sundar Madihally

---

Dr. R. Russell Rhinehart

---

Dr. Jim Smay

---

Dr. A. Gordon Emslie

---

Dean of the Graduate College

## TABLE OF CONTENTS

I. INTRODUCTION AND REVIEW OF LITERATURE .....	1
Tissue Engineering.....	2
Scaffold Material .....	3
Chitosan as scaffold material .....	5
Chitosan Biodegradation.....	7
PLGA .....	8
Scaffold Fabrication.....	9
II. HYPOTHESIS .....	11
III. MATERIALS AND METHODS.....	12
Sources of Chemicals.....	12
Polymer Solutions .....	12
Mixing Ratios.....	12
Method of mixing .....	13
Amount of stabilizer .....	13
Common recipe.....	14
Formation of scaffolds .....	14
Microstructure characterization .....	14
Porosity measurement.....	15
Macro-environment degradation.....	15
Cellular activity and degradation micro-environment .....	16
Statistical Analysis.....	16
IV. RESULTS .....	18
Obtaining stable emulsions .....	18
Optimizing Chitosan concentration for maximum porosity and structural stability.....	20
Method of emulsification.....	21
Effect of freezing rate on pore size and morphology.....	23
Comparison of effect of organic solvent on the pore size and shape.....	25
Effect of MW of PLGA on pore size and morphology.....	27
Effect of PLGA on Chitosan degradation.....	28
Effect of PLGA on cell spreading.....	30
Effect of PLGA on scaffold integrity.....	33
V. DISCUSSION .....	35
VI. CONCLUSIONS AND RECOMMENDATIONS .....	37

REFERENCES .....	38
APPENDIX I: EVALUATION OF PORE CHARACTERISTICS.....	39
APPENDIX II: SAMPLE RAW DATA.....	42
APPENDIX III: BOX PLOTS.....	43

## LIST OF TABLES

Table 1 Properties of Organic Solvents Used in Dissolving PLGA .....	19
--	----

## LIST OF FIGURES

Figure 1 Conceptual process for tissue engineering. ....	3
Figure 2 Chemical structure of chitosan. ....	5
Figure 3 Scaffold fabrication process. ....	6
Figure 4 Chemical structure of PLGA. ....	9
Figure 5 Stability of emulsions. ....	18
Figure 6 Effect of emulsion under SEM. ....	20
Figure 7 Scaffolds of chitosan-PLGA Blends. ....	21
Figure 8 Method of mixing doesn't influence scaffold properties. ....	23
Figure 9 Rate of cooling influences pore morphology. ....	24
Figure 10 Effect of organic solvent on the pore morphology. ....	26
Figure 11 Increased MW of PLGA may decrease pore size. ....	28
Figure 12 Degradation characteristics of chitosan/PLGA scaffolds. ....	29
Figure 13 Spreading characteristics of SMC. ....	31
Figure 14 Degradation Characteristics of blend and chitosan scaffolds at constant pH...	32
Figure 15 SEM micrographs of porous chitosan atop of a PLGA film. ....	34

## I. INTRODUCTION AND REVIEW OF LITERATURE

Approximately one half of the annual healthcare expenditure in the United States is due to tissue and organ failure <sup>1</sup>. Organs such as kidneys and heart as well as simple tissue such as skin or veins can be adversely affected by injury or disease to the point that their normal function is impeded. Traditionally patients would resort to surgical repair, prosthetics, drug therapy, or transplants; each with its own set of drawbacks <sup>2</sup>. Surgical repair is stressful and potentially dangerous to the patients and can require extended hospital stay as well as the need for follow up operations. In case of prosthetics, although many improvements have been made in recent years, there are still the fundamental issues that exist when introducing foreign material into the human body. Drug therapy can be successful in treating some diseases especially if the damage to the tissue or organ is not extensive; however there are unwanted side effects.

In many cases such as failed major organs the only viable option is a transplant from a donor. The vast majority of patients in need of major organ transplants face long waiting lists. According to the Organ Procurement and Transplantation Network there are currently over 88,000 patients on the waiting list for organ transplants; of those over 12,00 have been waiting for over 5 years <sup>3</sup>. Even after a transplant operation the patient faces immunosuppression and rejection difficulties and might not fully recover.

The difficulties associated with these treatment options have led scientists to pursue other alternatives to the general approach to the problem of damaged or diseased organs and tissues. One such alternative is the field of tissue engineering.

### *Tissue Engineering*

“Tissue engineering is the application of principles and methods of engineering and life sciences toward fundamental understanding of structure-function relationships in normal and pathological substitutes to restore, maintain, or improve tissue functions. In other words, tissue engineering involves the use of cells and extracellular components, either synthetic or natural, to create replacement, implantable parts to restore, maintain, or repair the function of damaged or diseased tissue and organs”<sup>4</sup>. The General approach to a specific application of engineered tissue involves first evaluating the conditions under which cells can produce tissue or organs. The most common method is to construct a porous 3-D structure onto which cells can attach and proliferate, commonly referred to as a tissue scaffold. This tissue scaffold should be biocompatible, sterilizable, and poses high enough surface area and void volume to allow for cell growth and differentiation as well as nutrient supply and waste removal<sup>5</sup>. Ideally scaffolds should also be designed to degrade at specific rates as to allow for more space for the cells to grow into and eventually the scaffold is completely and harmlessly removed from the patient. After the scaffold material has been prepared, cells are seeded onto the substrate and cultured *in vitro* for sometime, and finally the tissue scaffold is implanted at the necessary site *in vivo* (**Figure 1**). This is the most common method used by researchers and has yielded commercially available skin. Tissues such as bone, cartilage, blood



vessels, tendons, and others are also under investigation and have shown promise for success<sup>2</sup>. As the degree of complexity of the targeted tissue or organ increases, so do the required steps in the process. For example, stem cells and various growth and differentiation hormones may be included in the scaffold to yield the desired type and texture of cells; while scaffold architecture and *in vitro* fluid flow might be used to obtain the required cell orientation. As the science evolves, so will the methods used; however currently the general approach remains the same.

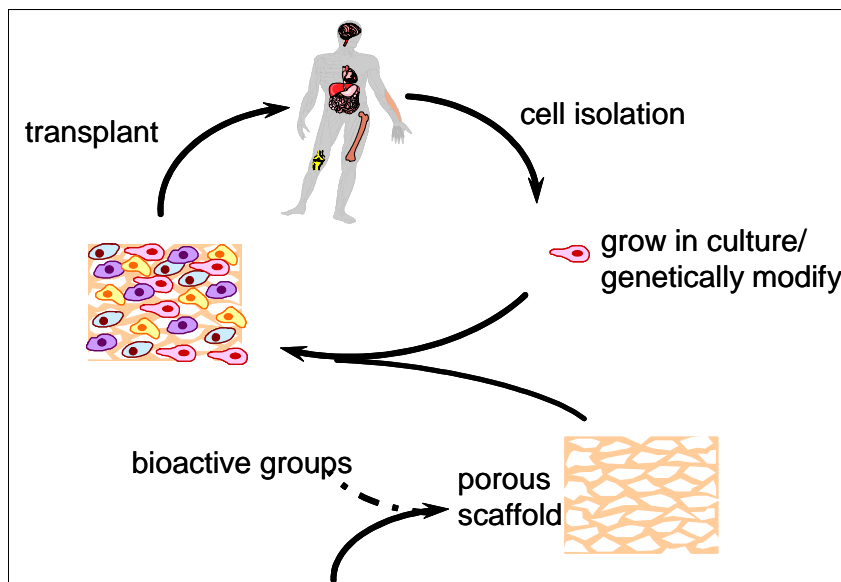


**Figure 1 Conceptual process for tissue engineering.**

### *Scaffold Material*

Since the tissue scaffold will mimic the function of the extracellular matrix (ECM) the design principles in tissue scaffold material have been governed by the function of the ECM. Extracellular matrix contributes greatly in signal transduction and provides a platform onto which cells can grow and repair in an injured site<sup>6</sup>. Any foreign material introduced to the body should above all be biocompatible and non-toxic. Furthermore, scaffolds should allow cell migration, adhesion, and proliferation; which inherently

requires a highly porous scaffold. Porosity also allows nutrients to reach the cells and waste removed from them. Previous research has shown that a porosity of at least 80-85% is required for scaffold success.

Also of importance is the degradation rate and nature of the degraded by-products. Since the goal is to completely remove the scaffold from the body the degradation process must be complete and obtained in a determined time frame. Ideally the degradation rate is synchronized with the rate of cell growth therefore not hindering the tissue regeneration process. The degradation products must also meet requirements for biocompatibility.

Another important factor in tissue scaffold design is the mechanical stresses that the scaffold must undergo at the implant site. Obviously various applications will require different mechanical strength properties; for example a blood vessel is under higher and more frequent stress than a portion of skin. Since the cells in the implant might not be able to mechanically support themselves for a period of time, the mechanical properties of the scaffold as it undergoes degradation is also critical.

The lack of suitable scaffold material has become a bottleneck in field of tissue engineering and is the subject of many research studies. Polymeric materials are ideal candidates for tissue scaffolds since they can be degraded through hydrolysis or enzyme-specific reaction *in vivo*<sup>7</sup>. Since a vast majority of biodegradable polymers do not satisfy all of the essential properties for a tissue scaffold material, numerous natural and synthetic polymers have been studied for tissue engineering scaffolds<sup>8</sup>. Examples of synthetic biopolymers include poly-lactic-acid (PLA), poly-glycolic-acid (PGA), and their co-polymer PLGA. Some of the natural biodegradable polymers include gelatin,

fibrin, chitin and its partially or completely deacetylated derivative chitosan. Most synthetic biodegradable polymers possess desirable mechanical strength and adjustable degradation rates but less than optimal cell compatibility while natural products such as collagen are inherently weak mechanically yet they exhibit excellent cell interactions<sup>9</sup>.

### *Chitosan as scaffold material*

Chitosan, the deacetylated version of chitin, has gained much attention as a biopolymer due to its biocompatibility, antimicrobial activity, and its low cost<sup>10,11</sup>.

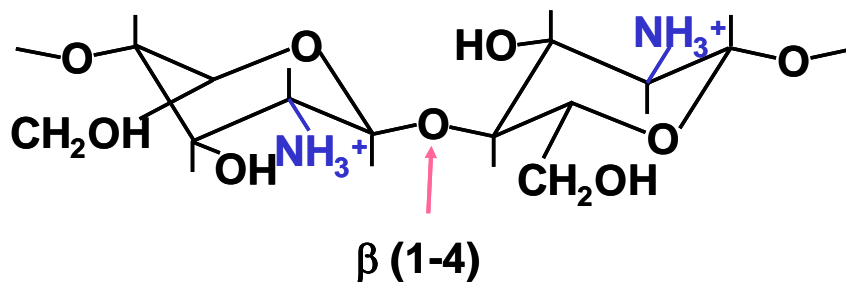


**Figure 2** Chemical structure of chitosan.

Chitosan (**Figure 2**) can form porous 3-D scaffolds through a controlled-rate freezing of chitosan solutions and subsequent lyophilization<sup>12</sup>. Ice crystals nucleate in solution during the freezing process and grow along the thermal gradients. During this process chitosan falls out of solution and is trapped between the ice crystals forming a honeycomb structure. At this time, if the solvent is allowed to melt it will re-dissolve the chitosan returning back to solution; therefore, lyophilization is used to remove the ice and creates a porous structure. Since the pore size is directly related to the size of the ice crystals, the mean pore diameter can be controlled by the rate of freezing. The orientation of the pores can also be controlled by directing the pathways of heat removal

during freezing (**Figure 3**). Controlled rate freezing technique generates an open pore structure, suitable for guiding cell ingrowth. Since Controlled rate freezing technique is carried out at low temperatures, it avoids the concern associated with the loss of biological activity of proteins due to thermal denaturation. Bioactive molecules such as mitogenic factors and therapeutic molecules can be incorporated during the fabrication process without altering their biological regulation.

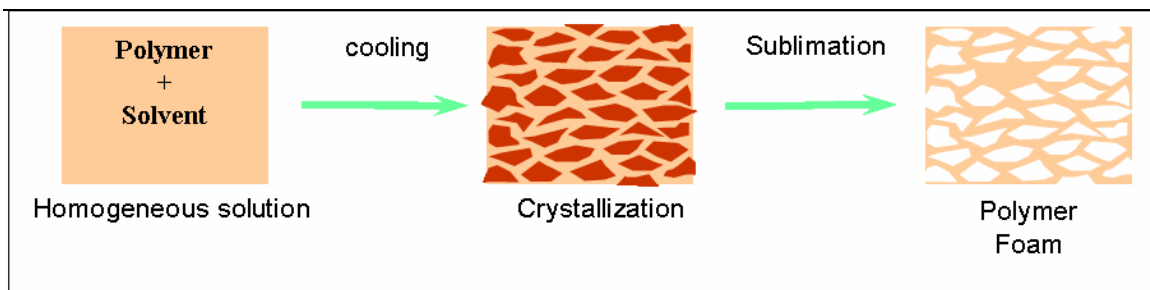


**Figure 3 Scaffold fabrication process.**

Chitosan scaffolds support the attachment, morphology, and proliferation of various kinds of cells, including chondrocytes, dermal fibroblasts, hepatocytes, and adrenal chromaffin cells<sup>4</sup>. Chitosan biocompatibility has been investigated by implanting porous chitosan scaffolds in mice and evaluating the subsequent histology. Results showed minimal inflammatory reaction to the chitosan scaffold<sup>13</sup>.

Chitosan has been combined with various biopolymers. *Mao, et al.*<sup>14, 15</sup> combined chitosan with gelatin to construct an artificial skin bilayer. While chitosan/calcium phosphate scaffolds have been used for bone regeneration<sup>4</sup>. Mixing chitosan with other biopolymers allows scientists to enhance its mechanical properties or cell-scaffold interactions.

Along with ease of processing and good cellular support for various cell types, chitosan also possesses desirable wound healing properties, antimicrobial activity, and biodegradability. Several clinical studies have shown that chitin-based products allow for faster healing of surgical wounds as well as reduced scarring. Chitosan is considered a primer upon which normal tissue is organized. Enhanced vascularization and a continuous supply of chitooligomers to the wound that enable the proper accumulation, assembly and orientation of collagen fibrils are properties exerted by chitosan in the rebuilding site <sup>4</sup>. Chitosan attacks the microbial cell wall which inhibits microbial activity. Chitosan has been investigated as a possible mechanism to prevent secondary infections or to prevent immunological rejections of transplants or implants.

#### *Chitosan Biodegradation*

As for any tissue scaffold candidate material, the degradation behavior of chitosan is of high importance. Biodegradable and nontoxic materials which are capable of support cellular activity are highly desirable. Various studies have shown that chitin and chitosan degrade in vivo via enzymatic hydrolysis by lysozyme. Lysozyme can be found throughout the body; however, the degradation rate is a function of the type of chitin, deacetylation method, and local pH.

It has been shown that with other factors being equal heterogeneously prepared chitosans were less susceptible to hydrolysis by lysozyme than homogeneously prepared chitosans <sup>16</sup>. Data suggest that there must be segments consisting of at least three consecutive N-acetyl sugar residues for lysozyme to be effective. These block segments are readily found in homogeneously prepared chitosans. Pangburn *et al* <sup>17</sup> report that

pure chitin is most susceptible to lysozyme while pure chitosan which has been 100% deacetylated cannot be degraded by lysozyme. It has been determined that the optimum pH for lysozyme to degrade chitosan is around 5.2<sup>18</sup>. Varum *et al*<sup>19</sup> showed that the initial degradation rate of lysozyme was 5 times higher at a pH of 4.5 than 7.

In tissue engineering applications it is important to minimize the exposure time between the scaffold and the host in order to minimize adverse affects. To utilize chitosan as a scaffold material its degradation rate must be maximized and controlled. While factors such as MW and the degree of deacetylation can be controlled prior to scaffold implantation, the pH of the implant site cannot.

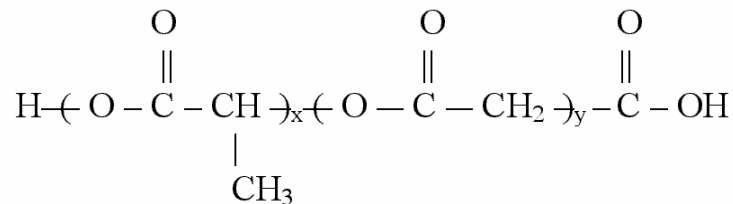
Therefore, it is desirable to locally reduce and maintain the pH of the implant site without causing side effects to the patient. The approach taken by the authors is to place a secondary polymer within the chitosan matrix that produces acidic byproducts during its own degradation. Thus, by controlling the secondary polymer's degradation rate we can control the pH in the chitosan scaffold and further increase and control chitosan's degradation rate. The requirements for this secondary polymer is that it will be biocompatible, proven safe for in vivo implantation, have tunable degradation rate, and degradation products are acidic but safe biocompatible components.

### *PLGA*

Poly-lactic-co-glycolic acid (PLGA) was chosen to be the polymer to be added into the chitosan matrix. PLGA has generated immense interest as a biomaterial due to its strong approval history, and its degradation has been studied during the past few decades. PLGA degrades via chemical hydrolysis of the hydrolytically unstable ester

bond (**Figure 4**) into lactic acid and glycolic acid which are non-toxic and biocompatible.

The degradation of PLGA is influenced by its Molecular Weight (MW), copolymer composition, crystallinity, and other structural characteristics<sup>20</sup>. A 50:50 copolymer ratio was chosen for these experiments because of its high degradation rate and various molecular weights were tested. However, when this copolymer is implanted alone it shows poor regulation on cellular activity, and scaffolds show structural instability due to swelling during degradation.



Poly(lactic acid-*co*-glycolic acid)

**Figure 4 Chemical structure of PLGA**

### *Scaffold Fabrication*

As previously stated controlled rate freezing and lyophilization can be used to obtain highly porous and tunable chitosan scaffolds. In order to incorporate PLGA in the chitosan scaffold via this technique both polymers must be present in solution prior to freezing. Since PLGA not readily soluble in water, the common method of lyophilization could not be applied without some modification. An emulsion system of organic solvent containing PLGA and aqueous solution containing chitosan is tested. In order to stabilize

the emulsion a natural emulsifier, 1,2-Dimyristol-sn-Glycero-3-Phosphocholine (DMPC), is used. DMPC is a biocompatible phospholipids found in egg yolks.



## II. HYPOTHESIS

The hypothesis is that by producing a chitosan scaffold with homogeneously dispersed pockets of PLGA we can take advantage of chitosan's good cellular activity while increasing its degradation rate. In order to achieve the desired homogeneous distribution, an emulsion system of an organic solvent containing PLGA in an aqueous solution of chitosan stabilized by DMPC was investigated. The method of controlled rate freezing and lyophilization would then be applied to this emulsion. However, the effect of introducing these changes on the pore morphology and pore distribution should be investigated. In particular, the method of emulsification, the amount and type of stabilizer, the type of organic solvent, and whether the new scaffold is cytotoxic. Small 3-D scaffolds were formed using controlled-rate freezing technique and subsequent lyophilization. Using these scaffolds, the relationship between porosity and concentration of each polymer were investigated. The microstructures of these scaffolds were analyzed using SEM and digital photo analysis. A four week long degradation study comparing the blended scaffolds and pure chitosan scaffolds in lysozyme solution and physiological conditions was conducted. Results show that a highly porous, homogeneous scaffold can be obtained and its pore size controlled. Preliminary results show that the scaffolds do not exhibit cytotoxicity and degradation of chitosan has increased in the presence of PLGA. The results of the study may help us evaluate the feasibility of producing lyophilized 3-D scaffolds containing chitosan and PLGA for tissue engineering.

### III. MATERIALS AND METHODS

#### *Sources of Chemicals*

50 to 190kD MW chitosan with 85% degree of deacetylation, DMPC (99% from egg yolk, 678 Da), and hen egg white (HEW) lysozyme (46,400 U/mg) ,were obtained from Sigma Aldrich Chemical Co (St. Louis, MO). 19kD 50:50 PLGA was obtained from Alkermes Inc., (Cambridge, MA) while 75kD and 160kD 50:50 PLGA were purchased from Birmingham Polymers (Birmingham, AL). All other reagents were from Fisher Scientific (Pittsburgh, PA).

#### *Polymer Solutions*

0.1 to 1% (wt/volume) chitosan solutions were prepared by dissolution in slightly acidic (0.2M acetic acid) solution. 1 to 10% (wt/volume) 50:50 PLGA solutions of various MWs were prepared by dissolving in chloroform, methylene chloride, DMSO, or benzene. 10% (wt/volume) DMPC solution was prepared in chloroform.

#### *Mixing Ratios*

Originally equal volume chitosan and PLGA solutions were mixed together; however this resulted in partial blending with excess PLGA solution (organic phase) separating out. In order to achieve uniform blending, the amount of PLGA solution was gradually decreased until a uniform, white, ad creamy emulsion was present after mixing. The final mixing ratio was set at 3:1 (aqueous:organic), and this ratio was used for all

subsequent experiments.

#### *Method of mixing*

After addition, the samples were capped and mixed by three different methods in order to investigate whether the amount of energy used in mixing had an effect on the scaffolds. The first method was to simply shake the vials containing the mixture by hand for about 20seconds. The second method was to place the vials on a mini-vortexer (Fisher Scientific) at 3200 rpm for 3 to 4 min. The third method involved sonication for 90 seconds at 50% amplitude by a 500 Sonic Dismembrator (Fisher Scientific). These methods were chosen because each presented a different mechanism for mixing. All these samples were used for scaffold formation and their properties analyzed.

#### *Amount of stabilizer*

Although mixing 3:1 chitosan to PLGA solution resulted in a creamy uniform emulsion, it lacked stability after few minutes (depending on the method of mixing) and the two phases would separate. In order to stabilize the emulsion long enough for the freezing process to take effect a natural stabilizer 1,2-Dimyristol-sn-Glycero-3-Phosphocholine (DMPC) was added to the organic phase prior to mixing. For accuracy the DMPC was first dissolved in chloroform (10% wt/volume) and then added volume wise to the PLGA solution. Thru a trial and error method, the minimum amount of DMPC solution required for stable emulsion was determined to be 10 $\mu$ L per 1 mL of PLGA. A discussion of this process is presented in the results section.

### *Common recipe*

Unless otherwise stated, blend scaffolds will refer to 3:1 chitosan solution to PLGA solution. Chloroform is used as the preferred PLGA solvent and the concentration of chitosan and PLGA are 0.3% (wt/v) and 3% (wt/v) respectively in their solutions. 10 $\mu$ L of 10% DMPC was added for every 1mL of PLGA solution prior to mixing via vortexing.

### *Formation of scaffolds*

0.3 to 8 mL portions of the blended emulsions were poured into flat bottomed 15 mm diameter Nalgen tubes. Freezing was accomplished by placing these tubes in a large (in excess of 1000 X the sample volume) ethanol baths equilibrated at temperatures of -20°C, -78°C, and liquid nitrogen naturally equilibrating at -196°C in order to achieve different cooling rates. After the samples frozen at -20°C and -78°C equilibrated at their respective temperatures, they were subsequently placed in liquid nitrogen prior to lyophilization so that all samples the same final temperature. All samples were lyophilized until dry using a Benchtop 6K lyophilizer (VirTis, Gardiner, NY).

### *Microstructure characterization*

Lyophilized scaffolds were sectioned at various planes, attached to sample stubs with carbon paint and sputter-coated with palladium prior to examination under a JOEL JXM 6400 Scanning Electron Microscope (SEM). Imaging was conducted at an accelerating voltage of 15 kV or 10 kV. Obtained digital micrographs were analyzed for pore area, major axis, minor axis and shape factor using image-analysis software (Sigma Scan Pro, SPSS Science, Chicago, IL). Shape factor is defined as  $4\pi \times \text{area} / \text{perimeter}^2$ ,

and when the number is closer to 1, the cell shape is closer to a circle. See Appendix 1 for more details.

#### *Porosity measurement*

Total volume was measured by determining the height and the diameter of the scaffolds. The scaffold was then placed inside a graduated cylinder with a pre-measured amount of absolute alcohol and the change in the volume of alcohol was measured once the scaffold was submerged, which corresponds to the volume of the solids in the scaffold. The porosity is thus approximated by:

$$Porosity = \frac{(TotalVolume - SolidVolume)}{TotalVolume} \times 100$$

#### *Macro-environment degradation*

A 3:1 (aqueous:organic) vortexed blend of 1% chitosan solution and 3% 160 kD PLGA solution was used to generate 2 mL emulsified scaffolds using chloroform as the organic solvent (frozen at -196°C). All of the scaffolds were neutralized and sterilized with ethanol prior to further processing. Half (n=32) of the samples were incubated in 10 mL of phosphate buffer saline (PBS) solution at 37°C and 5% CO<sub>2</sub> /95% air while the other half (n=32) were incubated in 10 mL of PBS containing 10 mg/L hen egg white (HEW) lysozyme solution and placed in the same conditions. Chitosan scaffolds without PLGA (n=64) were also prepared and used as controls by subjecting them to the same conditions as the blended scaffolds. The initial mass of the scaffolds were recorded and the pH of the buffer solution was recorded weekly. The medium was changed after the first week and once every two weeks thereafter.

### *Cellular activity and degradation micro-environment*

GFP-transfected canine bladder smooth muscle cells (SMC) were a kind gift from Dr. Bradley Kropp, Department of Urology, University of Oklahoma Health Science Center, Oklahoma City, OK and maintained following his protocol. The growth medium consisted of M199, supplemented with 10% calf serum, 100 U/ml and 100 µg/ml penicillin-streptomycin, 2.5 µg/ml amphotericin B, MEM amino acids, 3.56 gm/L HEPES, 0.5 gm/L bacteriologic peptone and 1gm/L dextrose.

Thin sheets of chitosan and PLGA-chitosan scaffolds were formed by freezing at -196°C. They were neutralized and sterilized in alcohol as described for the degradation study. Circular samples covering single wells in a 24-well-culture plate were cut and inserted into the wells. The cell suspension was seeded on these scaffolds at 30,000 cells/well. The cells were incubated under 5% CO<sub>2</sub> at 37 °C. Cultures were fed with fresh medium every 48 hours. Half (n=12) the samples were incubated with media containing lysozyme while the other half (n=12) were incubated under similar conditions without lysozyme. Pure chitosan scaffolds were also prepared and used as controls. Media was monitored for changes in pH and leached-out GFP-fluorescence. After one and three weeks, scaffolds were dehydrated using ethanol series and analyzed via SEM.

### *Statistical Analysis*

The distributions of pore sizes were plotted as box plots to show the 10<sup>th</sup>, 25<sup>th</sup>, 50<sup>th</sup>, 75<sup>th</sup> and 90<sup>th</sup> percentiles and the mean value (thick line within each box). Values that were outside 95<sup>th</sup> and 5<sup>th</sup> percentiles were treated as outliers. At least 50 pores were characterized for each condition from micrographs obtained by representative regions of

the scaffolds. A one-way analysis of variance (ANOVA) with 95% confidence interval was also used to evaluate the significant differences between various groups. See Appendix II for more detail.

## IV. RESULTS

### *Obtaining stable emulsions*

First, the amount of DMPC was optimized based on the minimum amount required to stabilize the emulsion for 10 to 30 min. This will allow the freezing process to take place while both polymers are uniformly dispersed. Various quantities of DMPC was added to 3:1 solvent ratios of water and organic solvents i.e., chloroform (**Figure 5A**), benzene, and methylene chloride.

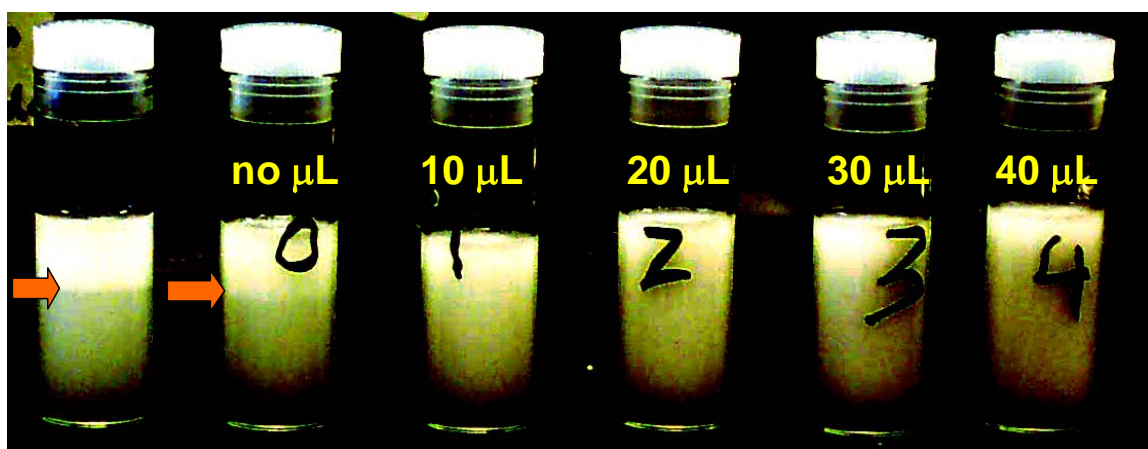


**Figure 5** Stability of emulsions.

Stability of the emulsion formed by hand mixing 3 mL water and 1 mL chloroform with various volumes of DMPC. Samples with no label contained no PLGA, and no DMPC. All other samples had 3% (wt/v) 19kD PLGA. Arrow indicates the phase separation region.

Upon mixing of chitosan solution and chloroform as control (**Figure 5** vial with no label) the solution separates in two phases (arrow). When PLGA is present but no DMPC (**Figure 5** vial labeled 0) better mixing occurs yet there is still not uniform dispersion especially as time passes. However when DMPC is added in 10 $\mu$ L, 20 $\mu$ L, 30 $\mu$ L, and 40 $\mu$ L (vials labeled 1, 2, 3, and 4 respectively) the emulsions are stable up to



30 min. No apparent difference could be observed between samples of various DMPC contents therefore the smallest amount of DMPC solution (10 $\mu$ L per 1mL PLGA solution) was used for all subsequent samples.

Stability of the emulsion was observed consistently in all the mixtures with different polymer contents. This stability was more prevalent in emulsions formed using benzene and chloroform solvents. Methylene chloride did not reach a stable emulsification state. In samples where stable emulsion was observed, an increase in the volume of the organic solvent resulted in organic solvent accumulating on the top or bottom of the emulsion, depending on the specific gravity of the organic solvent used (**Table 1**).

**Table 1 Properties of Organic Solvents Used in Dissolving PLGA.**

<b>Organic Solvent</b>	<b>Benzene</b>	<b>Chloroform</b>	<b>Methylene chloride</b>
Melting Point ( $^{\circ}$ C)	5.5	-63.5	-95.0
Boiling Point ( $^{\circ}$ C)	80.1	59.0	39.8
Vapor Pressure (mmHg)	100 at 26.1 $^{\circ}$ C	200 at 25.9 $^{\circ}$ C	400 at 24.1 $^{\circ}$ C
Specific Gravity(20 $^{\circ}$ C/4 $^{\circ}$ C)	0.879	1.48	1.32
Heat of Melting(cal/g)	22.64	47.01	12.94
Specific heat(cal/g. $^{\circ}$ C)	0.419(6-60 $^{\circ}$ C)	0.232(0 $^{\circ}$ C)	0.288(15-40 $^{\circ}$ C)

However, the observed stability of the emulsion could be due to unknown interactions between the three components. To understand this possibility, global changes in the thermal properties were analyzed using a Differential Scanning Calorimeter. These results (data not shown) indicated no significant changes in the

structure of three components suggesting no apparent interaction among the components.

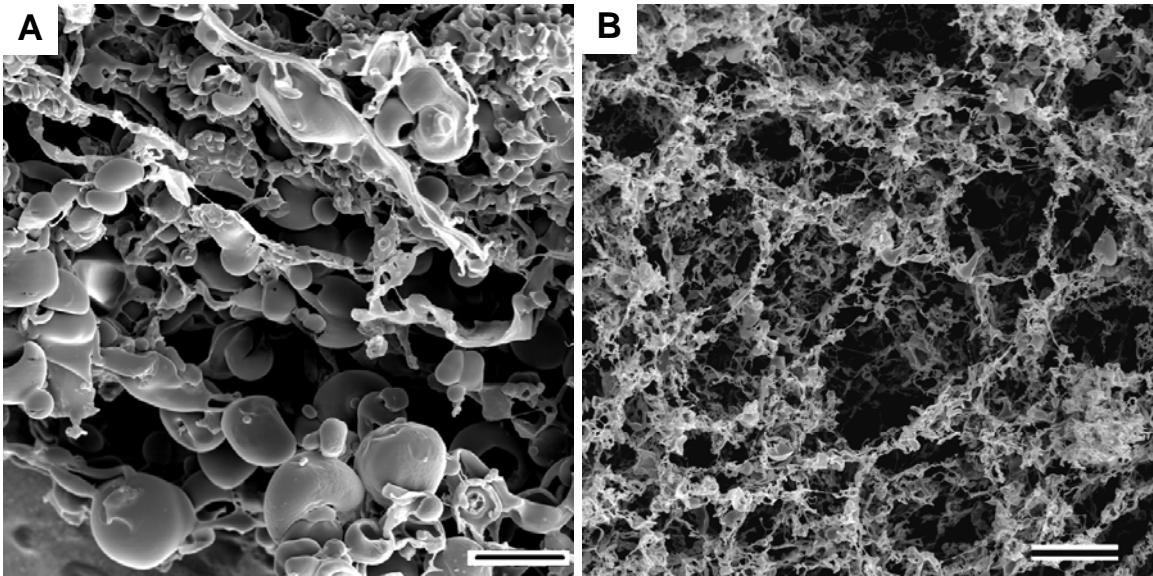


**Figure 6 Effect of emulsion under SEM.**

**Micrograph of a scaffolds in the absence of a stabilizer (Panel A). Micrograph of a scaffold in presence of a stabilizer (Panel B). The scale bars represents 100 µm.**

Scaffolds were formed with and without DMPC using controlled rate freezing and lyophilization. Micro architecture analysis using SEM showed globules of PLGA in the chitosan network in the scaffolds formed without the emulsifier (**Figure 6A**). On the other hand, addition of the emulsifier inter-dispersed (**Figure 6B**) the two components uniformly throughout the scaffold with the appearance of homogenous structure along with a texture different from pure chitosan scaffolds. This suggested that the mode of stabilization of the emulsion was sufficient to obtain a uniform blend *Optimizing chitosan*

#### *Optimizing Chitosan concentration for maximum porosity and structural stability*

Next, to understand the influence of blend compositions, cylindrical scaffolds were formed using 0.1% to 1% (wt/volume) chitosan solutions. Scaffolds formed from 0.3% chitosan solution showed porosity in the range of 95 to 98%. A direct relationship

between the concentration of chitosan to the porosity of the sample was observed, however, the concentrations did not affect the pore morphology. Increasing PLGA content from 2% to 6% (wt/volume) at a constant chitosan content of 0.3% (wt/volume), moderately decreased the porosity to 92-93%. Quantification of scanning electron micrographs showed that addition of PLGA to chitosan did not significantly affect the pore size distribution and the shape of the pores in the scaffolds (**Figure 7**). However, scaffolds formed with PLGA alone from the emulsions showed decreased pore area and diameter due to structural collapse. Based on these results, subsequent scaffolds used 0.3-1%(wt/volume) chitosan and 3-5% (wt/volume) PLGA.

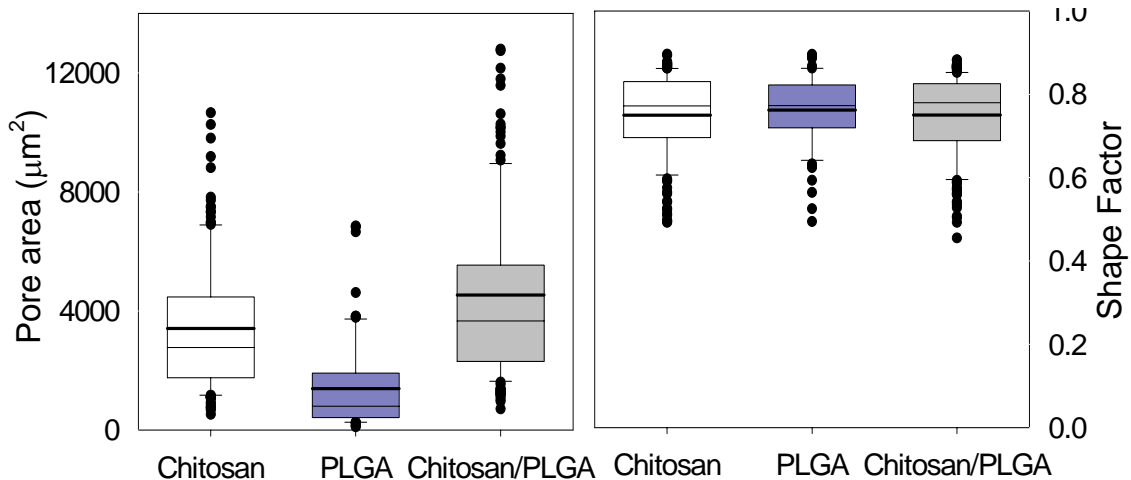


**Figure 7 Scaffolds of chitosan-PLGA Blends.**

**Box plot showing the distribution of pore area (Panel A) and the shape factor (Panel B) of the pores in the scaffolds.**

#### *Method of emulsification*

Since the method of combining PLGA with chitosan could determine the distribution of two phases, the method of mixing by sonication, vortexing and hand mixing were compared. These results showed that sonication for 90 sec alone produced

emulsions of the two components in the absence of the stabilizer although these emulsions showed phase separation within 10 min of the process. Nevertheless, adding the stabilizer to the emulsion significantly extended the stability. Next, these emulsions were frozen at an ethanol bath maintained at  $-78^{\circ}\text{C}$  and then lyophilized to obtain porous scaffolds. These results showed that emulsions formed after all the three mixing methods generated structurally stable scaffolds. Analysis of the scaffolds via SEM showed no significant difference between the methods of mixing i.e., sonication (**Figure 8A**), vortexing (**Figure 8B**), and hand mixing (data not shown) on the micro-architecture of the scaffold.

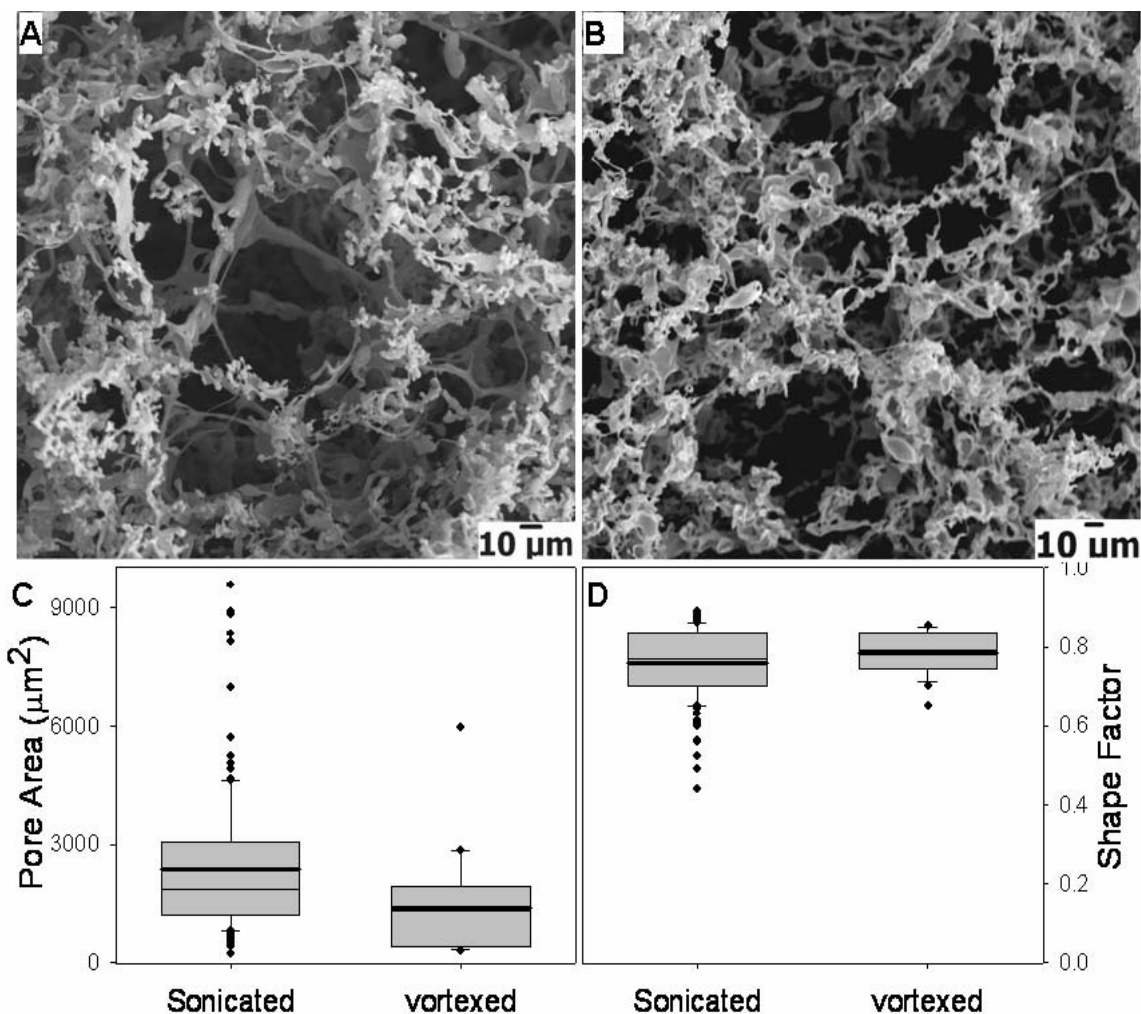


**Figure 8 Method of mixing doesn't influence scaffold properties.** Micrographs of scaffolds formed using 3% of 160 kD at  $-78^{\circ}\text{C}$  after sonication (Panel A) and after vortexing (Panel B) were characterized for pore sizes (Panel C) and shape factor (Panel D).

Further quantification of the micrographs showed (**Figure 8C and 8D**) no significant difference in pore area, pore diameter or the shape factor of these scaffolds. Thus vortexing was used in all the subsequent studies.

#### *Effect of freezing rate on pore size and morphology*

To better understand the influence of rate of freezing on microarchitecture of the blend scaffolds, samples were frozen and at various cooling rates. This was achieved by

constant temperature ethanol bath maintained at  $-20^{\circ}\text{C}$  and  $-78^{\circ}\text{C}$  or liquid nitrogen baths of  $-196^{\circ}\text{C}$ . These results showed that controlled rate freezing easily regulated the pore size distribution between  $2\ \mu\text{m}$  and  $300\ \mu\text{m}$  (**Figure 9A and 9B**), similar to pure chitosan scaffolds.

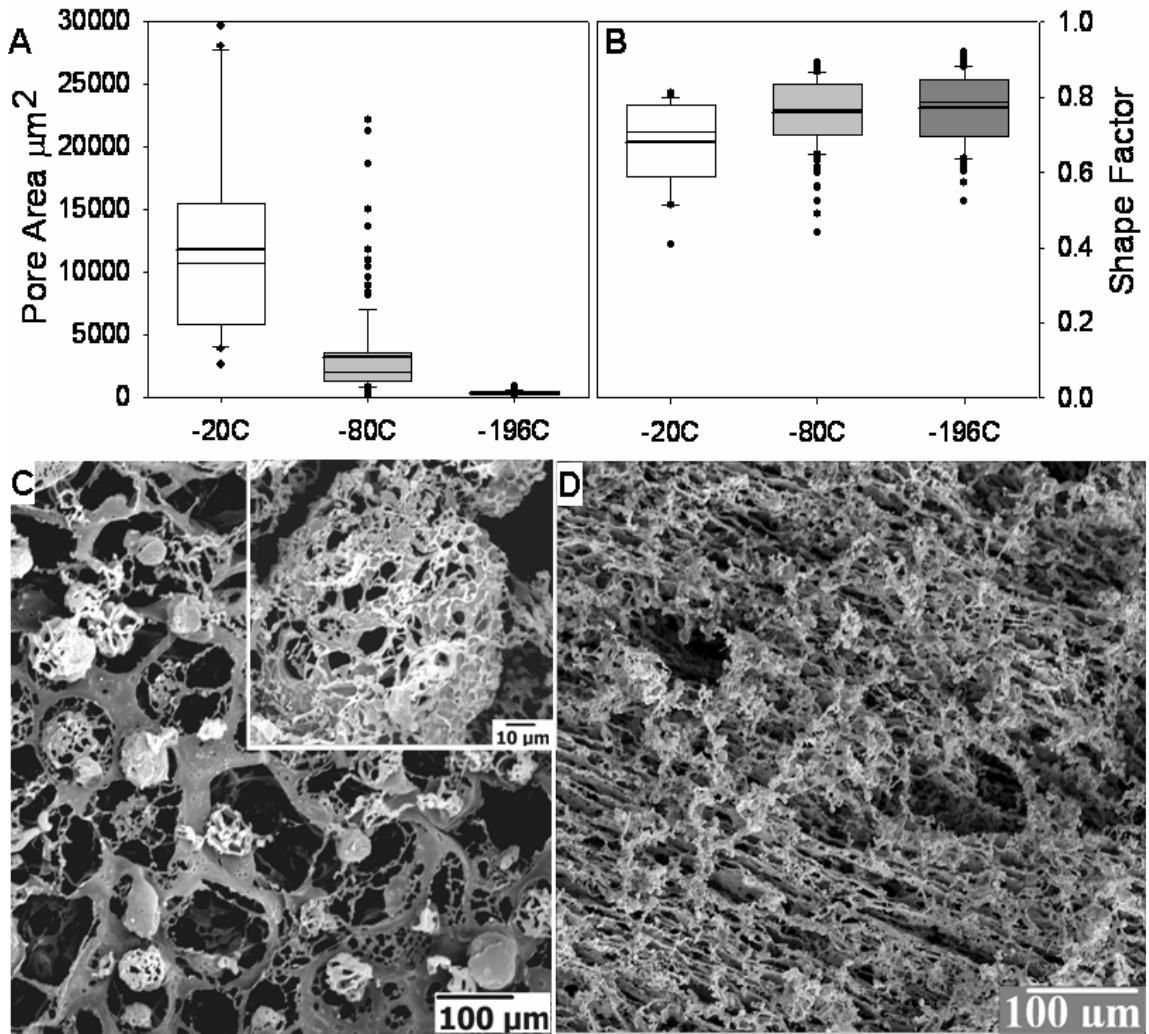


**Figure 9** Rate of cooling influences pore morphology. Scaffolds were characterized for pore size (Panel A) and shape factor (Panel B). Micrographs of scaffolds formed using 3% of 19kD after freezing at  $-20^{\circ}\text{C}$  (Panel C) and  $-196^{\circ}\text{C}$  (Panel D).

The lower heat transfer rate of  $-20^{\circ}\text{C}$  ethanol bath produced much larger pore sizes relative to samples frozen at the higher heat transfer rate present in the  $-78^{\circ}\text{C}$

ethanol baths. However, a careful observation of the scaffolds showed moderate phase separation and formation of globules in samples frozen at  $-20^{\circ}\text{C}$  (**Figure 9C**). This could be attributed to the physical characteristics of chloroform such as the melting point (shown in **Table 1**); when frozen at  $-20^{\circ}\text{C}$ , due to a) preferential cooling of water, b) reduced freezing rate, and c) no solidification of chloroform, resulted in phase separation. Nevertheless, due to subsequent cooling of samples at  $-196^{\circ}\text{C}$  resulted in crystallization of chloroform and formation of micro pores within the globules (see the inset picture in **Figure 9C**). Similar characteristics were also more prevalent in methylene chloride containing samples frozen at  $-20^{\circ}\text{C}$  or  $-78^{\circ}\text{C}$ . On the contrary, this was not observed in samples frozen directly at  $-196^{\circ}\text{C}$  (**Figure 9D**) or benzene containing samples. Further, when benzene was used as the organic solvent, freezing the samples at  $-20^{\circ}\text{C}$  did not show any phase separation due to the high melting point of benzene (**Table 1**).

#### *Comparison of effect of organic solvent on the pore size and shape*

Since the effect of rate of cooling was confounded by the physical properties of the organic solvents, influence of organic solvents alone on scaffold pore morphology was studied by freezing 1% 19kD PLGA dissolved in benzene, chloroform, or methylene chloride, and 0.3% chitosan at a constant temperature of  $-196^{\circ}\text{C}$ . The lower amount of 50:50 PLGA was set by the limited solubility  $<1.5\%$  (wt/volume) in benzene. These results showed that freezing samples at  $-196^{\circ}\text{C}$  produced relatively large pore sizes in scaffolds formed using chloroform (**Figure 10A**) and methylene chloride (data not shown) rather than benzene (**Figure 10B**) as the solvent. The addition of organic solvents further increased the pore areas (**Figure 10C**) than scaffolds formed with pure

water alone <sup>12</sup>.

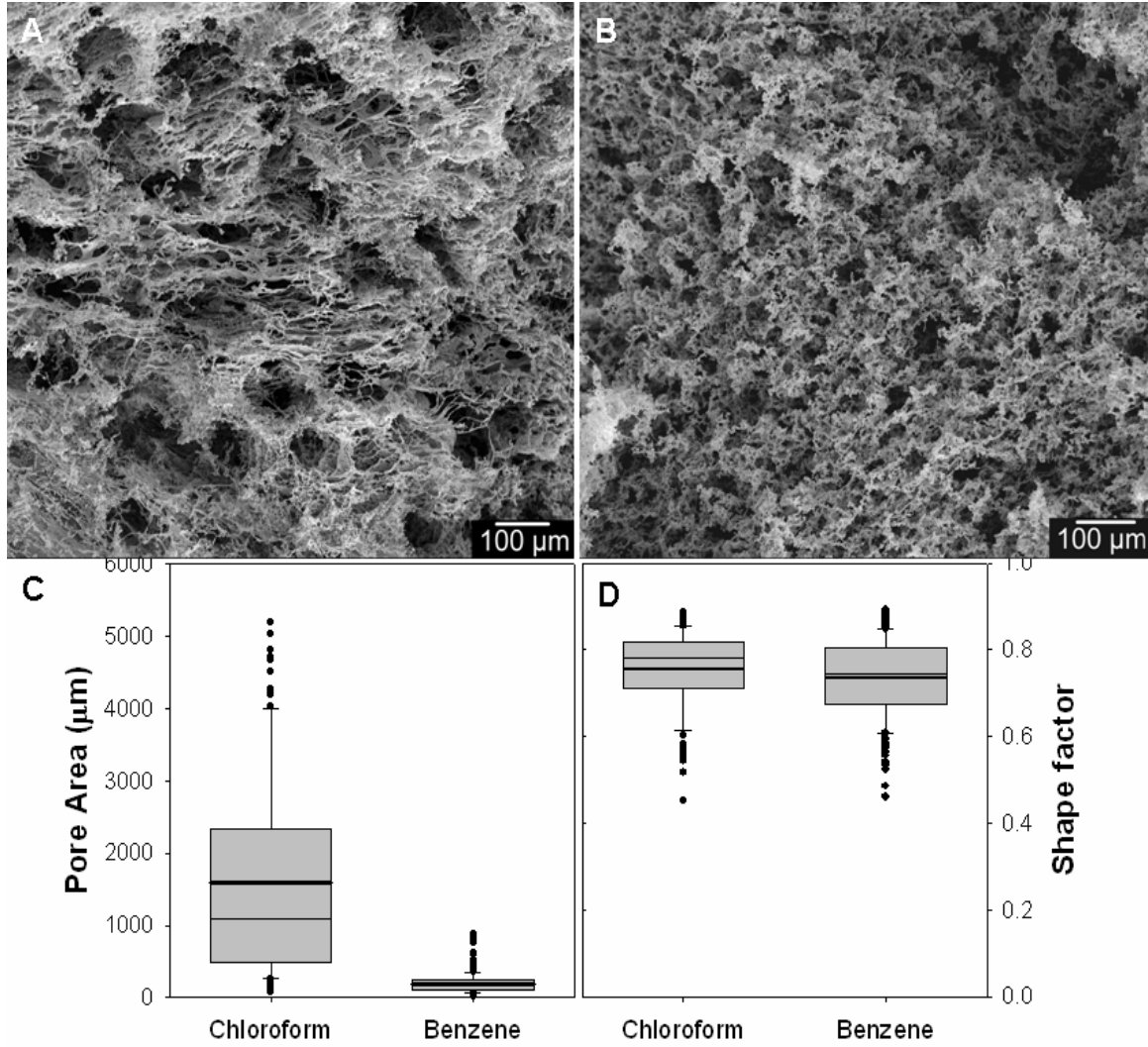


**Figure 10** Effect of organic solvent on the pore morphology. Micrographs of scaffolds formed after freezing at  $-196^{\circ}\text{C}$  using 1.5% of 19kD in chloroform (Panel A), and benzene (Panel B) were characterized for pore size (Panel C) and shape factor (Panel D).

There was no significant difference in the shape of the porous structure in all the organic solvents and the average of shape factor varied from 0.75 to 0.8 (**Figure 10D**). Previous research has shown that dimethyl sulfoxide (DMSO) can be used to combine PGA (polyglycolide) and chitosan utilizing a freeze drying process <sup>21</sup>. However we were not able to produce larger scaffolds than the reported 500μm thick samples. This is due



to the low vapor pressure of DMSO which makes it difficult to fully remove the solvent in a lyophilizer at room temperature unless the scaffold is thin and flat. Limitations in emulsifying methylene chloride, reduced solubility of 50:50 PLGA in benzene, and difficulties in lyophilizing DMSO, led to choosing chloroform as the organic solvent in subsequent experiments.

#### *Effect of MW of PLGA on pore size and morphology*

To understand how the MW of PLGA influences the pore morphology, 3% 19kD, 75kD and 160 kD PLGA were blended with 0.3% chitosan. Although a change in the viscosity of the PLGA solution was noticeable, no significant differences were observed during emulsification process. To understand the influence on scaffold architecture, samples were frozen at  $-78^{\circ}\text{C}$  (**Figure 11A and 11B**) or at  $-196^{\circ}\text{C}$  and then lyophilized.

These results showed that the increase in MW of PLGA decreased the pore sizes of the scaffold (**Figure 11C**) but the pore shapes were not affected (**Figure 11D**). The decrease was more significant in samples frozen at  $-78^{\circ}\text{C}$  than at  $-196^{\circ}\text{C}$ ; when samples were frozen at  $-196^{\circ}\text{C}$  only a trend towards decreased pore sizes with no significant differences were observed.

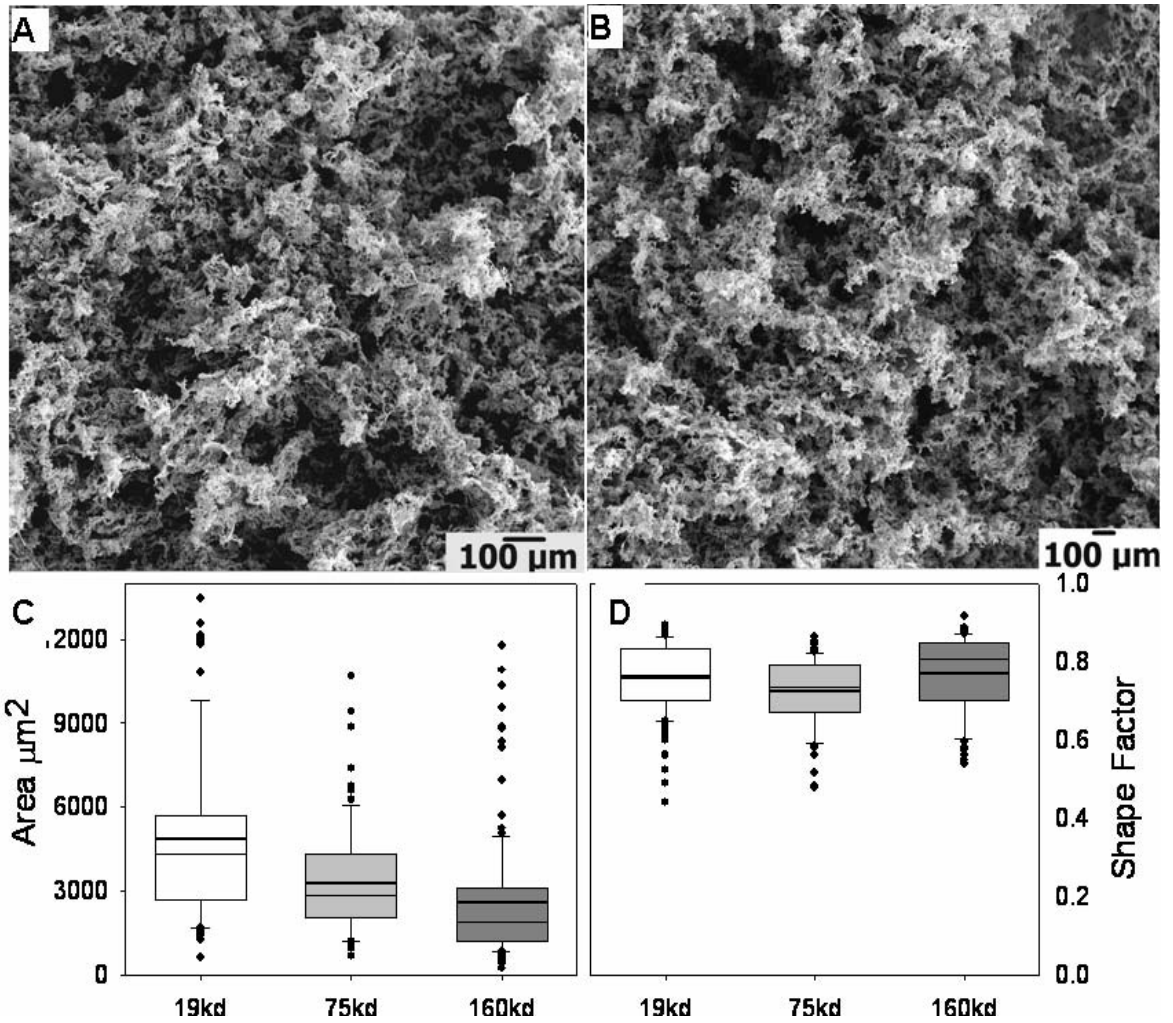


**Figure 11 Increased MW of PLGA may decrease pore size.** Increased MW of PLGA may decrease pore size. Micrographs of scaffolds formed after freezing at -78°C using 3% of 75 kD (Panel A), and 160 kD (Panel B) PLGA were characterized for pore sizes (Panel C) and shape factor (Panel D).

*Effect of PLGA on Chitosan degradation*

To test the hypothesis that introducing PLGA enhances the degradation of chitosan, cylindrical scaffolds formed using chloroform were incubated in 10 mL of PBS

containing 10 mg/L lysozyme. The concentration of lysozyme was chosen to mimic the physiological circulating levels in the plasma which is 4-13 mg/L<sup>22</sup>. Results (**Figure 12A**) show that only chitosan/PLGA scaffolds incubated in the presence of lysozyme structurally collapsed by week four.

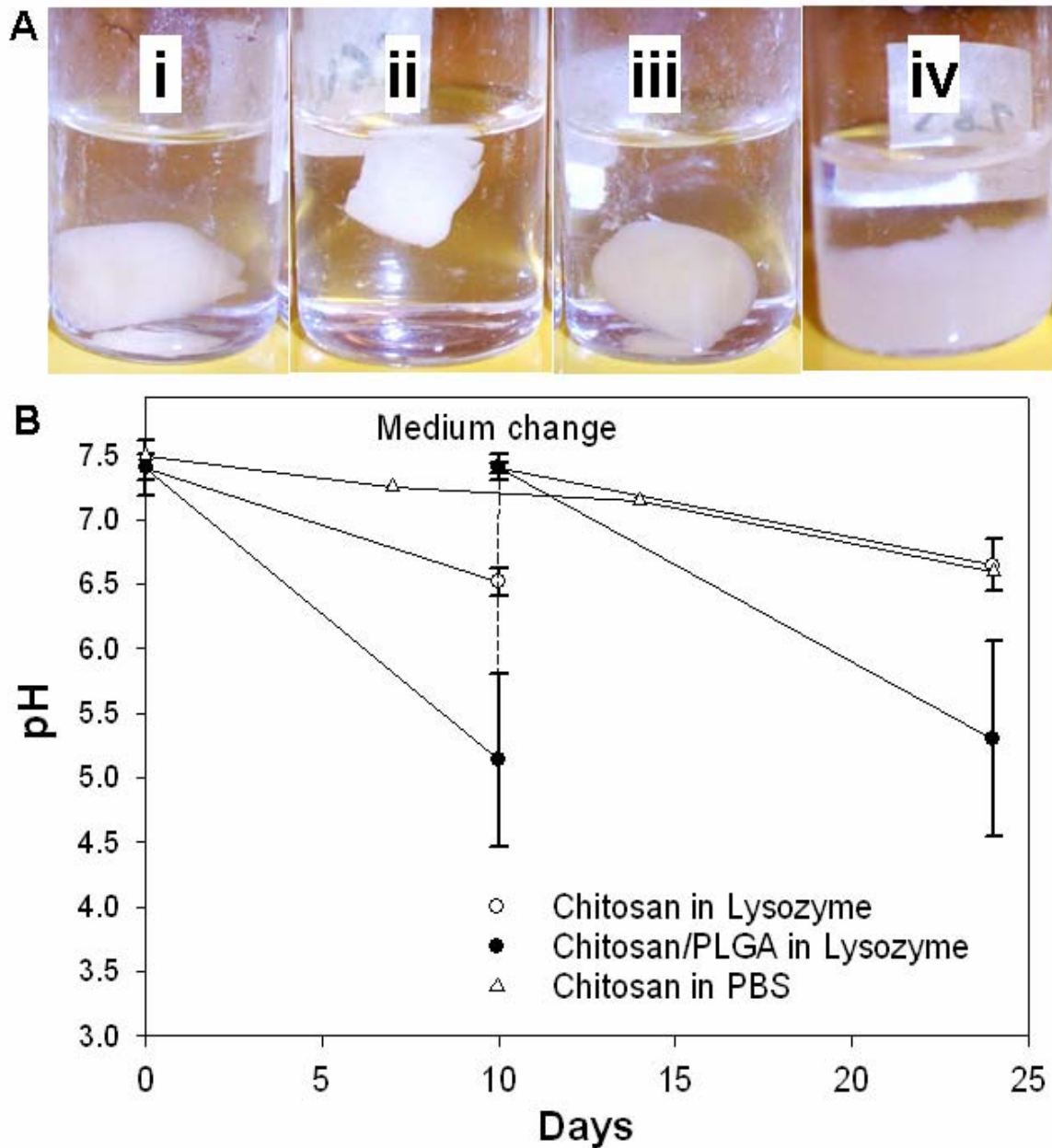


**Figure 12** Degradation characteristics of chitosan/PLGA scaffolds.

**Panel A.** Photographs taken after 24 days i) chitosan in PBS, ii) chitosan-PLGA PBS, iii) chitosan in PBS containing lysozyme, and iv) chitosan-PLGA in PBS containing lysozyme. **Panel B.** Media pH changes.

All other samples did not show significant alterations in the dimensional changes unlike pure PLGA scaffolds which show swelling during degradation<sup>23</sup>. To understand the reason, media pH was monitored. These results (**Figure 12B**) indicated that chitosan/PLGA scaffolds incubated in presence of lysozyme showed a significant reduction in pH relative to all other conditions, probably due to the synergistic degradation of both chitosan and PLGA which form acidic products. This drop in pH increases the activity of lysozyme in addition to the possibility of dissolving chitosan.

#### *Effect of PLGA on cell spreading*

The increased degradation with drop in pH of the macroenvironment cannot be expected *in vivo* because the acid will be readily cleared. In addition, altered pH could be cytotoxic to cell survival. Therefore cellular activity and the degradation characteristics of the scaffolds under conditions where the global pH of the solution is held constant via frequent buffer changes were studied. When SMCs were cultured, the measured fluorescence of the media showed no significant increase in the GFP-fluorescence relative to control or chitosan, suggesting no toxicity. However, when cell spreading was compared (**Figure 13**), cells on PLGA-chitosan showed reduction in cell spreading area and were more circular in morphology.

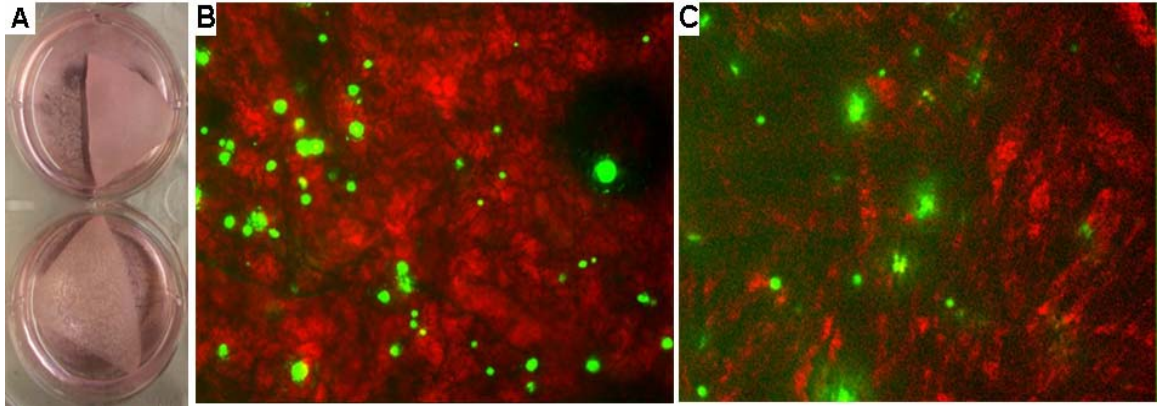


**Figure 13 Spreading characteristics of SMC.**

**GFP-transfected canine bladder smooth muscle cells seeded on lyophilized scaffolds at 30,000 cells/well. Panel A. Photographs showing thin scaffolds. Panel B. Chitosan scaffold. Panel C. 160 kD emulsified PLGA/chitosan scaffold.**

Analysis of the degradation characteristics showed an increase in the amount of chitosan degraded in the presence of PLGA as compared to pure scaffolds. Day zero SEM micrographs of pure chitosan scaffolds (**Figure 14A**) showed a porous structure underneath the skin layer. Blend scaffold (**Figure 14D**) showed a similar structure but with more porous skin layer. After one week, without the presence of lysozyme, chitosan and blend scaffolds (**Figure 14B and 14E**) showed negligible degradation of the top layer. However, in the presence of lysozyme, the blend scaffolds (**Figure 14F**) show significant decrease in the skin layer than pure chitosan scaffolds (**Figure 14C**). Chitosan scaffolds did not show significant degradation in the presence of lysozyme even after three weeks (data not shown) and was similar to week one samples. However, the blend scaffolds after 3 weeks (**Figure 14G and 14H**) show significant degradation of the polymers and the pore wall structure appeared to be collapsed.

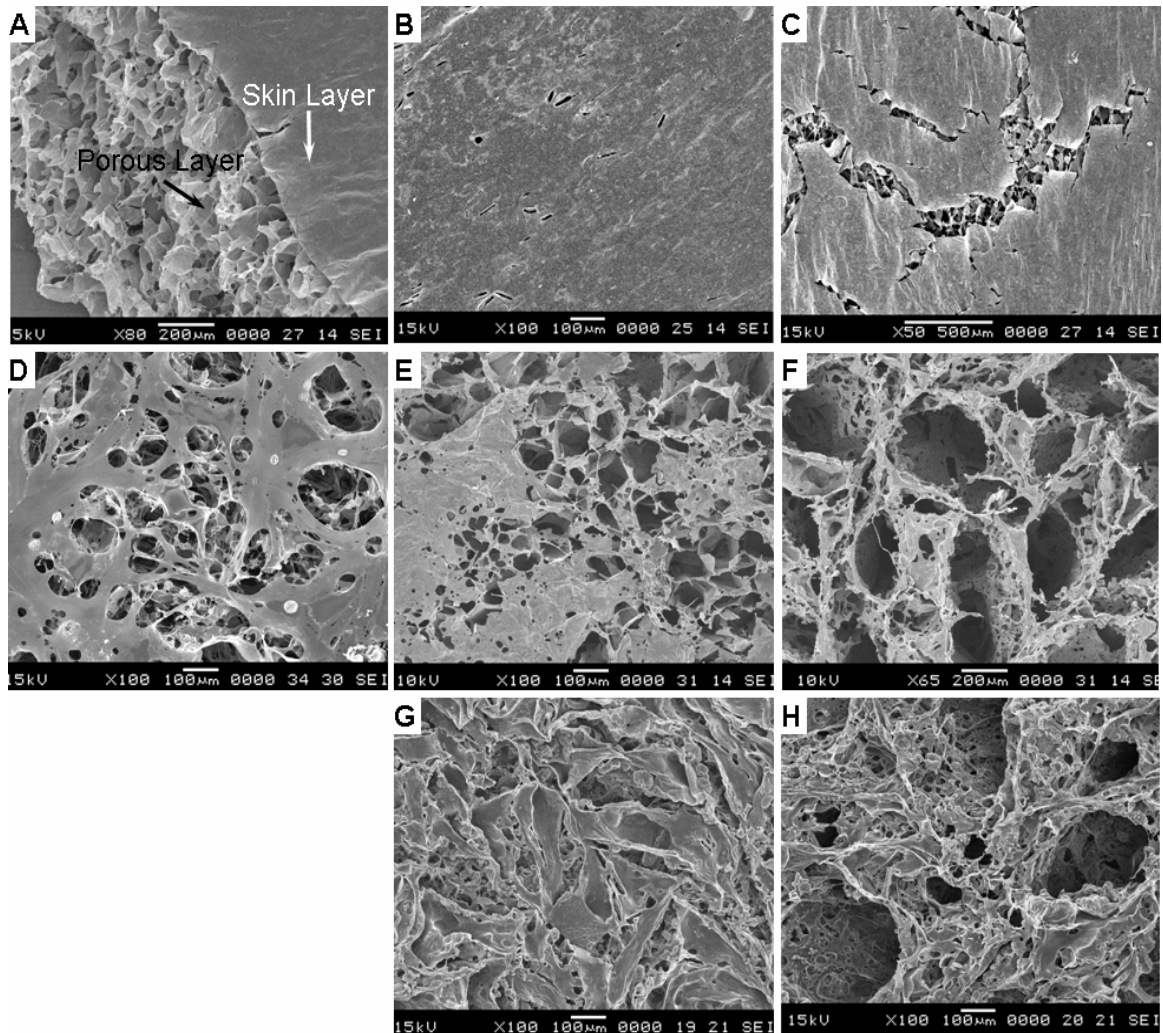


**Figure 14 Degradation Characteristics of blend and chitosan scaffolds at constant pH.** SEM micrographs of lyophilized scaffolds. Panel A. Day 0 Chitosan. Panel B. Week 1 chitosan with no lysozyme. Panel C. Week 1 chitosan with lysozyme. Panel D. day 0 blend. Panel E. week 1 blend without lysozyme. Panel F. Week 1 blend with lysozyme. Panel G. Week 3 blend without lysozyme. Panel H. Week 3 blend with lysozyme.

The media was changed on a daily basis and the pH of the removed media was measured. Results show no significant change in pH in all the samples, indicating a constant pH. Studying the increased deterioration of the skin effect in the blend scaffold as opposed to pure chitosan scaffolds shows that the presence of PLGA can potentially enhance degradation in physiological conditions.

### *Effect of PLGA on scaffold integrity*

It was believed that by introducing PLGA into the chitosan scaffold would result in a mechanically stronger scaffold than chitosan alone because PLGA is stronger than chitosan. This was not the case as the emulsified blend scaffolds were weaker than pure chitosan. In order to take advantage of PLGA's stronger mechanical properties it must be connected throughout the scaffold. To achieve such structure an alternate fabrication technique is proposed for future study. This technique suggests first forming a layer of PLGA film via evaporation then freeze drying a thin aqueous layer containing chitosan on top. SEM micrographs of such scaffolds show an open pore structure on the surface (**Figure 15A and 15D**) and a smooth continuous PLGA film on the bottom (**Figure 15B and 15C**). This structure allows PLGA to provide the backbone for the scaffold while the chitosan is responsible for cell interaction; at the same time due to the proximity of the two polymers the same enhanced degradation characteristics from emulsified scaffolds can be expected. The mechanical properties of this scaffold depend on the thickness of the PLGA film.

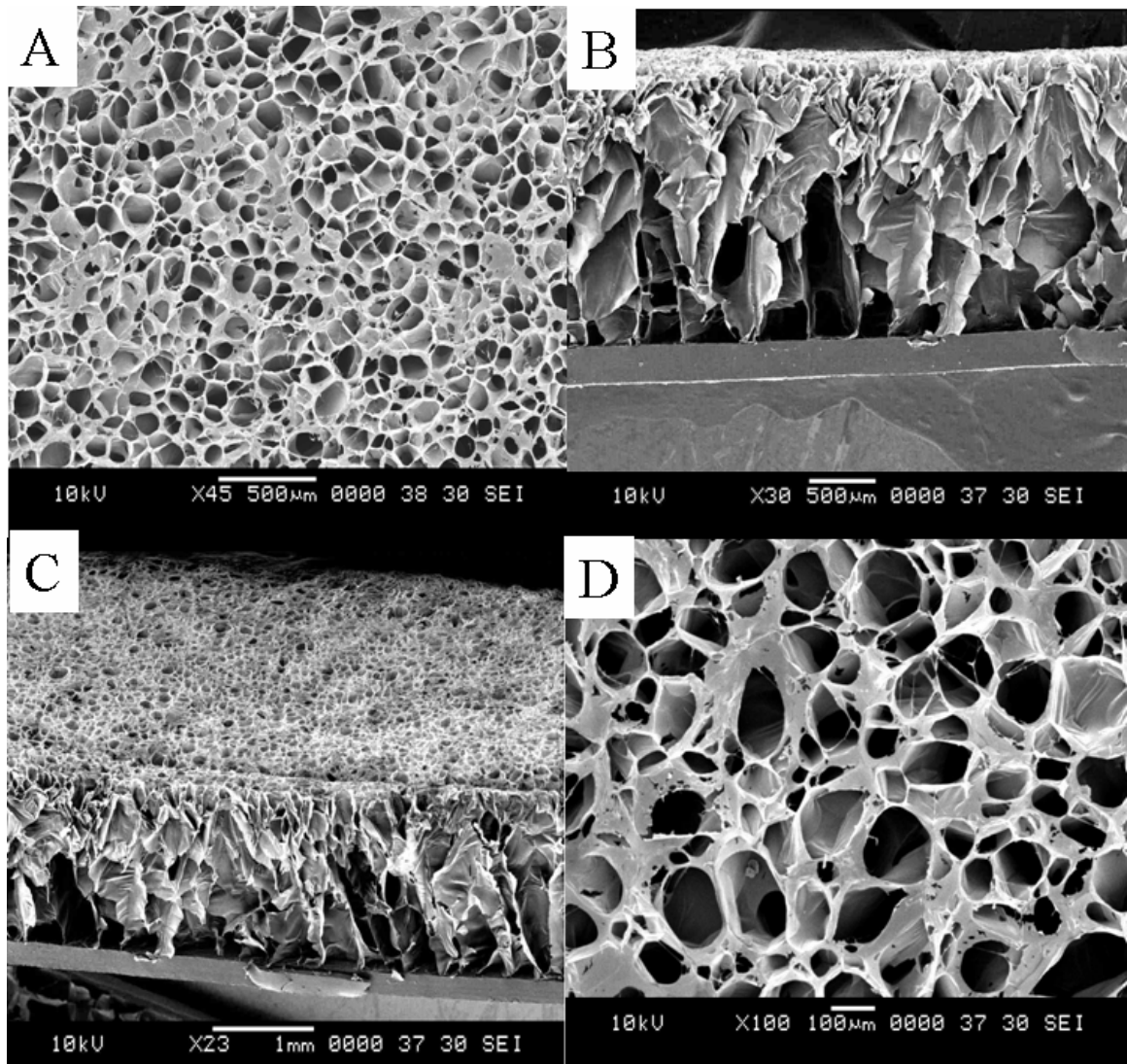


Figure 15 SEM micrographs of porous chitosan atop of a PLGA film. Top view (panel A and Panel B). Vertical cross sections (panel B and panel C).



## V. DISCUSSION

This study evaluated the blending of chitosan with 50:50 PLGA in the emulsification mode using DMPC as the stabilizer. An emulsion system was used to homogeneously disperse PLGA within the chitosan scaffold. This was done to prevent chemical changes to chitosan which might affect its desirable properties such as cell attachment and survival. Highly porous three dimensional scaffolds were obtained with no apparent chemical interaction between chitosan and PLGA. From visual observation, it was evident that the PLGA solution was dispersed in the form of micelles in the aqueous phase. This notion was further confirmed from the general structure of the scaffolds under SEM which resembled chitosan scaffolds in their overall microarchitecture. In the presence of DMPC, emulsions were stable for long enough time that was sufficient for the freezing process to take place.

Analysis of the prepared scaffolds showed that the freezing temperature influenced pore size, similar to pure chitosan scaffolds<sup>12</sup>, but MW of PLGA as well as the type of organic solvent also influenced the pore morphology. Of the three organic solvents used, benzene and chloroform emulsions were more stable than methylene chloride. Other organic solvents with sufficient synthetic polymer solubility can also be used, if necessary. However, the solvent should have high enough vapor pressure at room temperature (**Table 1**) to allow complete lyophilization. Reduction in chitosan concentration resulted in increased porosity up to 95%, however, scaffolds showed structural instability at very low (0.3%) chitosan concentrations. Blending PLGA with chitosan resulted in highly porous scaffolds. This system is not exclusive to chitosan and

PLGA combination alone and can be used for any two biopolymers where the solvents are aqueous and organic.

The degradation results showed that chitosan scaffolds containing PLGA have an enhanced lysozymal degradation rate. This effect can be attributed to the acidic environment created by release of lactic and glycolic acids during the degradation of PLGA. Further results show that this increase in degradation is still evident even if the global pH of the scaffold is held constant indicating that the local pH changes are responsible for enhanced degradation effect resulting in open pore morphology. Previous research has shown that lysozyme is much more active in acidic conditions than neutral, which this degradation study confirms.

Cellular activity of SMCs on these scaffolds showed no cytotoxic effects. However, a reduction in cell spreading area suggests a possible reduction in cell colonization. In a separate study, cell adhesion, cell proliferation, alteration in the cytoskeletal organization of endothelial cells and fibroblasts were studied and the fate of DMPC have been extensively studied<sup>24</sup>. These results show a reduction in cell proliferation and the internalization of DMPC. This suggests a need for improving the cellular activity by blending cytoadhesive polymers such as fibronectin or collagen into these scaffolds. Furthermore, preliminary mechanical property analysis indicates a reduction in the break stress and strain values relative to chitosan<sup>25</sup> and needs detailed analysis. An alternative fabrication technique is proposed in order to take advantage of PLGA's superior mechanical properties.

## VI. CONCLUSIONS AND RECOMMENDATIONS

In summary, this study demonstrated that chitosan and PLGA can be blended to obtain uniform, porous, 3-D scaffolds. These scaffold exhibits faster degradation than pure chitosan scaffolds. Using 3:1 ratio (volume/volume) of chitosan solution to PLGA solution (chloroform) and freezing in a  $-196^{\circ}\text{C}$  bath showed better characteristics in the pore size, homogeneity of scaffold, ease of processing, degradation, and cell culture. Future studies investigating the detailed degradation kinetics of chitosan in the presence of PLGA needs to be conducted as well as investigating the thermodynamics of the freezing process. Also of interest is whether the blended scaffolds containing PLGA exhibit the same swelling at the implant site as pure PLGA scaffolds<sup>23</sup>.

## REFERENCES

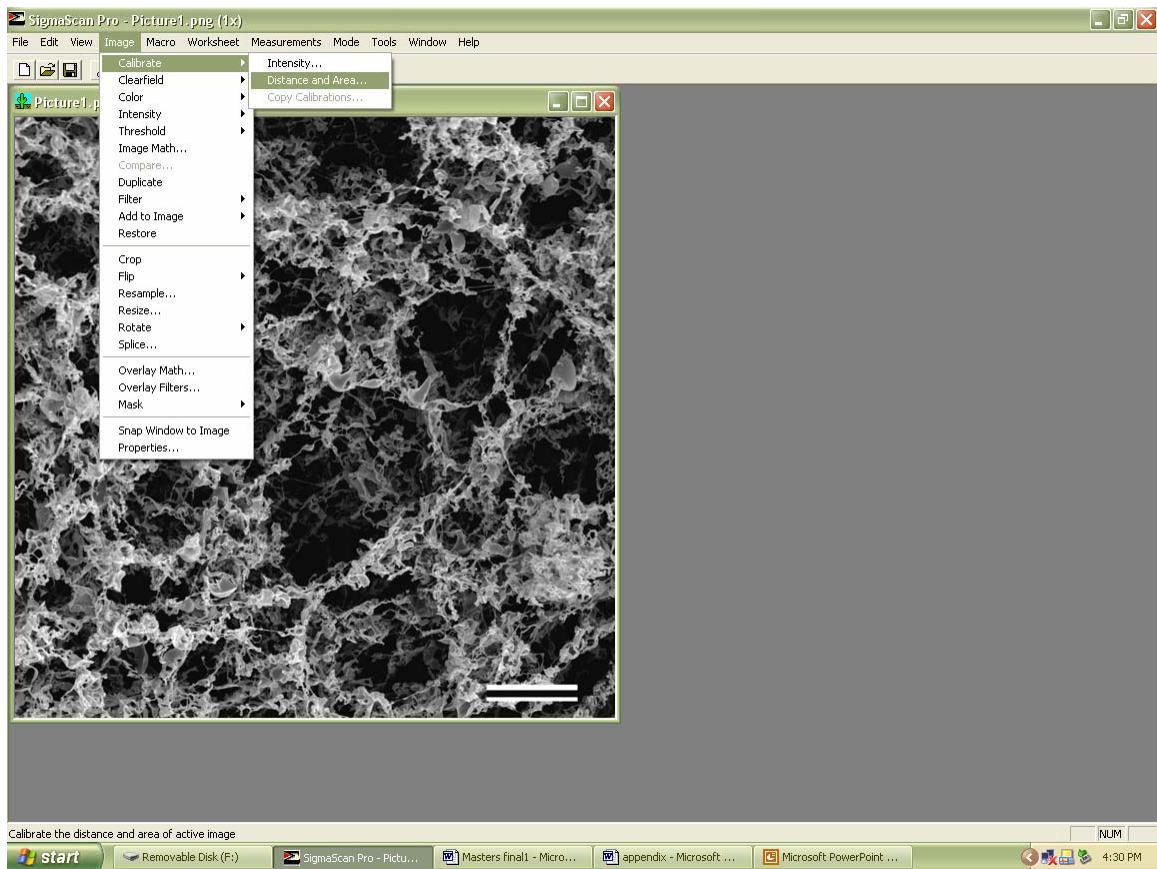
1. Lewis, R. *The Scientist* **Jul 14, 1995**, 9.
2. Nettles, D. L. Evaluation of Chitosan as a Cell Scaffold Material for Cartilage Tissue Engineering. Mississippi State University, 2001.
3. Department of Health and Human Services, H. R. a. S. A., Healthcare Systems Bureau, Division of Transplantation, Rockville, MD; United Network for Organ Sharing, Richmond, VA; University Renal Research and Education Association, Ann Arbor, MI. *2004 Annual Report of the U.S. Organ Procurement and Transplantation Network and the Scientific Registry of Transplant Recipients: Transplant Data 1994-2003*.
4. Ravi Kumar, M. N. V., et al. . *Chemecal Reviews* **2004**, *104*, 6017-6084.
5. Paige, K. T., Vacanti, C. A. *Tissue Engineering* **1995**, *1*, 97-106.
6. Lutolf, M. P.; Lauer-Fields, J. L.; Schmoekel, H. G.; Metters, A. T.; Weber, F. E.; Fields, G. B.; Hubbell, J. A. *PNAS* **2003**, *100*, 5413-5418.
7. Mi, F.-L.; Tan, Y.-C.; Liang, H.-F.; Sung, H.-W. *Biomaterials* **2002**, *23*, 181-191.
8. *Nat Biotechnol* **2000**, *18 Suppl*, IT56-8.
9. Tomihata, K.; Ikada, Y. *Biomaterials* **1997**, *18*, 567-575.
10. Muzzarelli RAA, J. C., Gooday GW (eds.). **1986**.
11. Chandy T, S. P. *Biomat., Art. Cells, Art Org* **1990**, *18*, 1 -24.
12. Madihally, S. V., and Mathew, H. W. T. *Biomaterials* **1999**, *20*, 1133-1142.
13. VandeVord, P. J.; Matthew, H. W.; DeSilva, S. P.; Mayton, L.; Wu, B.; Wooley, . H. *J Biomed Mater Res* **2002**, *59*, 585-90.
14. Mao, J. S.; Zhao, L. G.; Yao, K. D.; Shang, Q. X.; Yang, G. H.; Cao, Y. L. *J. Biomed. Mater. Res. Part A* **2003**, *64*, 301.
15. Mao, J. S.; Zhao, L. G.; Yin, Y. J.; Yao, K. D. *Biomaterials* **2003**, *24*, 1067.
16. Shigemasa, Y.; Saito, K.; Sashiwa, H.; Saimoto, H. *Int J Biol Macromol* **1994**, *16*, 43-9.
17. Pangburn, S. H.; Trescony, P. V.; Heller, J. *Biomaterials* **1982**, *3*, 105-8.
18. Davies, R. C.; Neuberger, A.; Wilson, B. M. *Biochim Biophys Acta* **1969**, *178*, 294-305.
19. Nordtveit, R. J.; Varum, K. M.; Smidsrod, O. **1996**, *29*, 163-167.
20. Wu, L.; Ding, J. *Biomaterials* **2004**, *25*, 5821-5830.
21. Wang, Y. C.; Lin, M. C.; Wang da, M.; Hsieh, H. J. *Biomaterials* **2003**, *24*, 1047-57.
22. Henry, J. B., *Clinical Diagnosis and Management by Laboratory Methods*. 18 ed.; Saunders: Philedphia, 1991; p 1371.
23. Agrawal, C. M.; Athanasiou, K. A. *J Biomed Mater Res* **1997**, *38*, 105-14.
24. Huang, Y.; Seiwe, M.; Madihally, S. V. *Biotechnology/ Bioengineering* **2005**, *Under revision*.
25. Sarasam, A.; Madihally, S. V. *Biomaterials* **2005**, (*in press*).

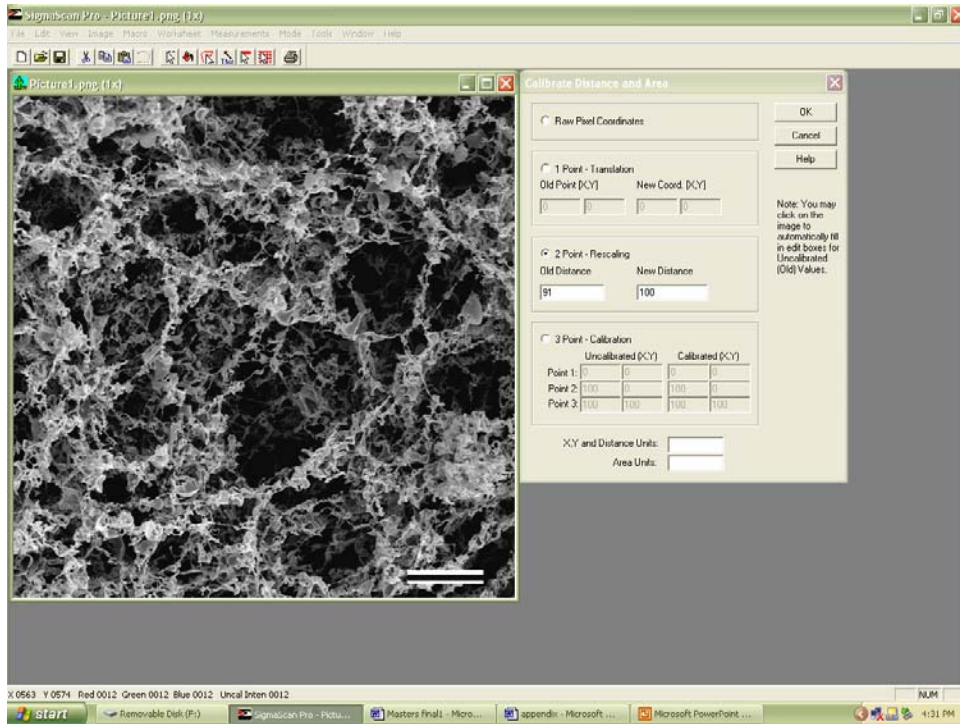
## APPENDIX I: EVALUATION OF PORE CHARACTERISTICS

**Step 1:** Obtain digital image via Scanning Electron Microscope (SEM)

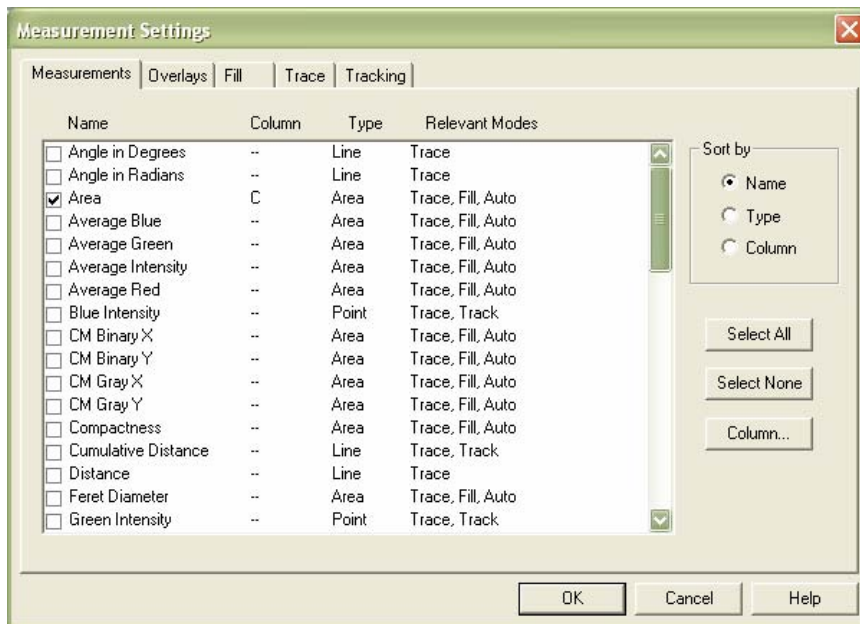
**Step 2:** Open image in Sigma Scan Pro

**Step 3:** Calibrate using 2-point calibration and the scale bar of SEM image (see the 2 figures below)





**Step 4:** Go to Measurements→Settings and select Area, Major axis, Minor Axis, and Shape Factor.

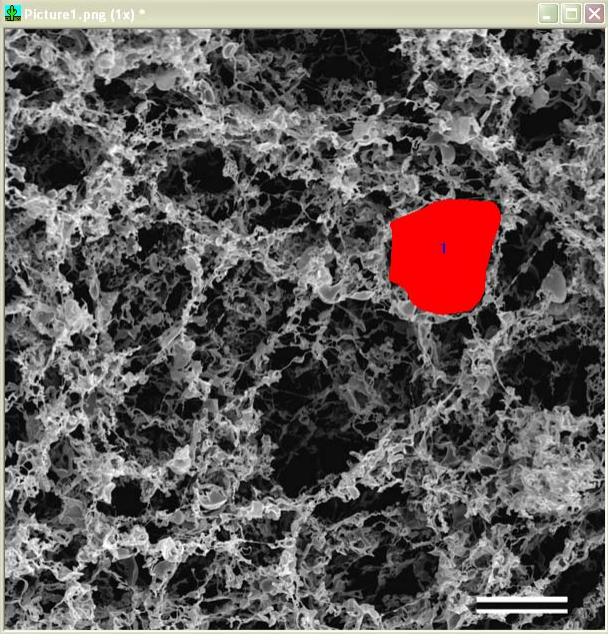


**Step 5:** Go to Mode→and select Trace Measurement Mode. Use the cursor to highlight the edges of a pore on the image. A worksheet will appear with the recorded measurements.

SigmaScan Pro - Worksheet2 \*

File Edit View Image Macro Worksheet Measurements Mode Tools Window Help

Picture1.png (1x) \*



Worksheet2 \*

A1   142.962767376458				
	A	B	C	D
	Maj Len	Min Len	Area	S Factor
1	142.96277	127.03601	12068.591	0.7965208
2				
3				
4				
5				
6				
7				
8				
9				
10				
11				
12				
13				
14				
15				
16				
17				
18				
19				
20				
21				
22				
23				

Cal X:0657.143 Y:0613.187 Red:0118 Green:0118 Blue:0118 Uncal:Inter:0118

Masters final1 - Microsoft Word

NUM

## APPENDIX II: SAMPLE RAW DATA

Sample raw data used to produce FIGURE 8.

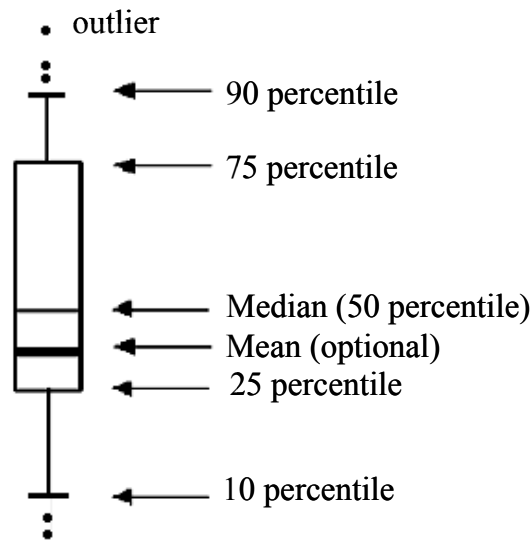
Area(micrometer <sup>2</sup> )		Major Length(micrometers)		Minor Length(micrometers)		Shape Factor	
Sonicated	Vortexed	Sonicated	Vortexed	Sonicated	Vortexed	Sonicated	Vortexed
4235.511	1280.618	95.2611	59.71716	70.39434	27.88959	0.679109	0.721117
1303.67	489.1277	45.2975	34.6405	39.92696	17.64466	0.874892	0.741195
2032.025	487.4223	66.76814	33.16277	37.83124	21.92139	0.795922	0.723012
3736.715	369.8525	90.75908	23.63713	49.71222	21.13875	0.764713	0.849083
881.3944	388.7191	35.71176	23.882	32.05228	23.29151	0.88303	0.848553
894.1477	313.0219	35.88987	22.26514	34.8482	21.04146	0.866889	0.651031
732.6059	311.2453	37.83124	29.92411	33.20318	14.77612	0.660811	0.698939
724.1037	367.8629	34.60336	28.63912	26.61797	17.70497	0.890627	0.782442
498.7955	648.7476	29.7598	32.26842	22.89764	28.49515	0.805958	0.810051
1136.46	339.9005	49.08111	24.56081	32.16262	17.28097	0.735551	0.833448
610.7411	481.542	35.01047	29.9514	24.27932	23.10619	0.677706	0.792953
569.6472	403.6952	30.1148	31.77521	27.14511	18.67764	0.821318	0.733577
1149.214	1574.436	44.173	54.72715	33.85823	36.58183	0.783045	0.790891
1493.553	2130.783	59.10149	70.88661	30.1148	42.18245	0.729872	0.749342
1582.826	2851.423	49.03779	72.30939	43.89948	48.69288	0.855059	0.812125
2474.139	2823.843	99.45295	70.38911	35.5128	54.5199	0.559521	0.818168
1309.338	2548.043	72.31079	73.06824	22.99029	44.61181	0.490348	0.800278
1190.307	5959.075	42.92019	107.908	39.57046	74.89613	0.85745	0.765442
1799.632	1359.431	74.01519	57.91453	31.44978	28.87265	0.64386	0.712466
980.5867	1681.495	38.75635	62.96358	35.79103	32.56529	0.809589	0.766524
1480.799	1510.676	58.62	54.06106	30.90437	38.15123	0.605259	0.7988
3723.962	1411.922	97.1173	49.49028	57.4603	37.08699	0.613746	0.831665
2393.368	1564.947	67.02234	58.57137	48.63155	33.86439	0.784651	0.778442
1402.862	2009.786	54.52462	56.60942	32.38216	46.44861	0.719466	0.852225
1912.994	1732.206	62.85449	64.80878	42.06987	36.78591	0.807397	0.780119
742.5252	2108.541	33.83729	61.44754	26.75073	43.84744	0.855352	0.853938
2039.11	800.9555	66.76814	35.32483	36.67102	32.26549	0.773969	0.848838
3524.16	613.5039	100.1982	31.45691	48.97996	23.95232	0.60448	0.847381



## APPENDIX III: BOX PLOTS

The box plot is a graphic display of the data that shows set's lowest value, highest value, median value and the size of the first and third quartile range. It is a quick method for determining the basic shape of a distribution and is also useful in detecting outliers.

These plots originate from the work of Tukey (1977).



### The Five Number Summary Box Plot.

**Variations on the box-plot** Sometimes the whiskers on the box-plot have a different methods of constructions, however, the hinges are always computed as the 25<sup>th</sup>, 50<sup>th</sup>, and 75<sup>th</sup> percentiles.

outliers may be identified using an outlier detection rule and are displayed using asterisks or some other character.

whiskers extend to 10<sup>th</sup> and 90<sup>th</sup> percentiles;

whiskers also identify other percentiles

the **thick** line corresponds to the mean.

median is the **thin** in the box

it is easy to compare groups by constructing side-by-side box plots as shown below.

$q_{25}$  = lower quartile, 25%of the data lie below this value

$q_{50}$  = median, 50%of the data lie below this value

$q_{75}$  = upper quartile, 25%of the data lie above this value

VITA

Aliakbar Moshfeghian

Candidate for the Degree of

Master of Science

Thesis: EMULSIFIED CHITOSAN-PLGA SCAFFOLDS FOR TISSUE

ENGINEERING

Major Field: Chemical Engineering

Biographical:

Personal Data: Born in Shiraz Iran, On march 24 1980, son of Mahmood and Sedi

Education: Graduated from Stillwater High School, Stillwater Oklahoma in may 1998; received Bachelor of Science degree in Chemical Engineering from Oklahoma State University, Stillwater, Oklahoma in May 2003. Completed the requirements for the Master of Science degree with a major in Chemical Engineering at Oklahoma State University in December 2005.

Experience: Worked in food service, remodeling, and marine engine factory as an undergraduate; employed by Oklahoma State University, Department of Chemical Engineering as an undergraduate and graduate research and teaching assistant; Oklahoma State University, Department of Chemical Engineering, 2003 to present.

Professional Memberships: American Institute of Chemical Engineers

Name: Aliakbar Moshfeghian

Date of Degree: December 2005

Institution: Oklahoma State University

Location: Stillwater, Oklahoma

Title of Study: EMULSIFIED CHITOSAN-PLGA SCAFFOLDS FOR TISSUE  
ENGINEERING

Pages in Study: 45

Candidate for the Degree of Master of Science

Major Field: Chemical Engineering

Scope and Method of Study: This study evaluated the formation of chitosan-50:50 poly-lactic-co-glycolic acid (PLGA) blend matrices using controlled rate freezing and lyophilization technique. An emulsion system was used in the presence of 1,2-Dimyristoyl-sn-Glycero-3-Phosphocholine (DMPC), a cellular component, as a stabilizer.

Findings and Conclusions: Blended scaffolds showed an open pore morphology and homogenous inter-dispersion of PLGA and chitosan. Forming emulsions after dissolving PLGA in chloroform, benzene, or methylene chloride indicated better emulsion stability with benzene and chloroform. Scaffolds formed by freezing at  $-20^{\circ}\text{C}$ ,  $-78^{\circ}\text{C}$  and  $-196^{\circ}\text{C}$  from these emulsions showed significant influence of the solvent and freezing temperature on the microarchitecture of the scaffold. By controlling the concentration of chitosan, scaffolds with greater than 90% porosity were attained. Since the two polymers degrade by different mechanisms, formed scaffolds were analyzed for degradation characteristics for four weeks in presence of 10 mg/L lysozyme. The degradation results showed that chitosan scaffolds containing PLGA have an enhanced lysozymal degradation rate. This effect can be attributed to the acidic environment created by release of lactic and glycolic acids during the degradation of PLGA. When cellular activity of GFP-transfected smooth muscle cells were analyzed, no apparent cytotoxicity was observed. However, the cell spreading area decreased. In summary, these results show promising potential in tissue engineering.

ADVISER'S APPROVAL: Dr. Sundar Madihally

---